JOURNAL OF MATERIALS SCIENCE 8 (1973) 427–438

Deterioration of impermeable alumina tubes in inert atmospheres at elevated temperatures

B. C. H. STEELE, M. A. WILLIAMS*
Metallurgy Department, Imperial College, London, UK

The deterioration of commercial impermeable alumina tubes when exposed to inert atmospheres at elevated temperatures (~1300° C) has been monitored using solid state electrochemical oxygen meters. The inability to maintain low oxygen partial pressures within the tubes was attributed to the development of porosity at elevated temperatures in the surface skin of the inner wall. Examination of samples by light and scanning electron microscopy, together with chemical analysis, indicated that the porosity was associated with a decrease in the impurity content. Thermodynamic evaluation confirmed that the relevant quantities of SiO_2, CaO, MgO could be removed as volatile species generated by the low oxygen partial pressures. The calculations also suggested that the formation of volatile species could result in significant contamination of samples undergoing heat-treatment in these alumina tubes.

1. Introduction

Physico-chemical measurements and the preparation of many materials at high temperatures often necessitate the use of commercial impermeable sintered alumina tubes. It is well known [1, 2] that such tubes can rapidly deteriorate at high temperatures (>1600° C) resulting in the development of porosity and eventual mechanical failure. It is usual therefore to design apparatus so that the effects of these undesirable properties are minimized. For example, furnaces incorporating at least two alumina tubes are often specified [3] to reduce the permeation of the atmosphere into the reaction tube.

Most of the evidence for the deterioration of alumina tubes has been obtained from material exposed to vacuum conditions [1, 2] and very high temperatures (1600 to 1700°C). There have been occasional comments [4], however, that impermeable alumina tubes can also deteriorate rapidly at much lower temperatures (<1400° C) when exposed to atmospheres imposing low oxygen chemical potentials within the reaction tube. Chemical reactions produced by the low oxygen potentials can be responsible for the formation of volatile species and the consequent development of porosity. These low oxygen potentials can be generated by appropriate gas buffer systems (H_2/H_2O or CO/CO_2 mixtures) or by purified "inert" gases such as argon, nitrogen, or helium and the precise chemical reactions associated with the deterioration will of course be influenced by the relevant system selected for the atmosphere control. The present investigation is concerned with the use of purified argon, and is particularly relevant to those situations involving the high temperature preparation and characterization of materials in inert atmospheres. The application of solid oxide electrolyte monitors for the continuous measurement of oxygen chemical potentials is also reported, and recommended for those investigations which require precise control of the oxygen content of the atmosphere.

2. Experimental techniques and results

2.1. High temperature apparatus

The apparatus incorporating the impermeable alumina tube was designed to investigate the thermodynamic properties of oxycarbide systems and has been described in an earlier report [5] on the uranium oxycarbide phase. The basic features are shown in Fig. 1. The impermeable

---

*Now at Anglesey Aluminium Metals Ltd, Penthos, Holyhead, Anglesey.

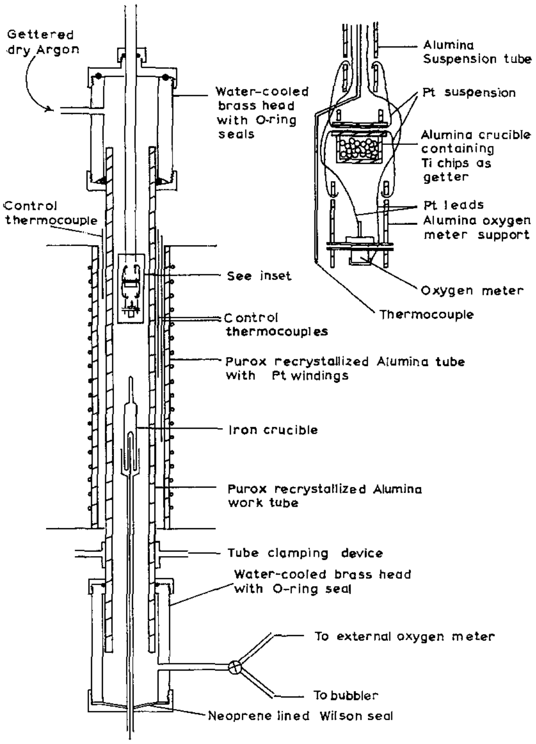

Figure 1 Furnace assembly incorporating alumina tube under examination.

alumina tube under examination served as the reaction tube in a vertical temperature gradient furnace fitted with three independently controlled Pt 20% Rh windings. Using "O" ring seals, water-cooled brass attachments were fixed to the ends of the alumina tube to allow either controlled atmosphere or vacuum operation. Other seals enabled a closed iron crucible, which contained the reactants relevant to the oxycarbide system under investigation, to be pushed into the hot zone and subjected to an appropriate temperature profile. It should be emphasized that the pure iron container fitted into an alumina crucible which prevented the iron container from touching the walls of the alumina reaction tube. Finally the electrical connections to a series of thermocouples, and the oxygen monitor situated in the upper part of the reaction tube, passed through the brass end assemblies via Neoprene or Araldite seals.

The design of the oxygen monitor has been described previously [6, 7] and essentially consists of a closed zirconia-yttria capsule incorporating a high-temperature glass-ceramic seal. The capsule contained an appropriate internal metal/metal oxide reference electrode (Fe/FeO for this investigation) together with an external platinum electrode to monitor the oxygen chemical potential of the gases introduced into the reaction tube. A similar device contained in small adjacent furnace was used to monitor the gases leaving the reaction tube.

It was obviously important to maintain a low oxygen chemical potential within the reaction tube to prevent oxidation and eventual disintegration of the pure iron container. Hydrogen could not be used as this gas would rapidly diffuse through the walls of the iron container and thus interfere with the oxycarbide equilibration experiment as well as producing embrittlement of the iron. Accordingly an inert atmosphere was maintained within the reaction tube using argon which had been purified by removal of CO_2 (Sofnolite), moisture (silica gel and magnesium perchlorate), and oxygen using titanium chips heated to 750°C.

The normal operating procedure was to test the apparatus for vacuum tightness before the furnace was switched on, and if satisfactory the purified argon was then introduced into the reaction tube and allowed to flow through the apparatus at 100 ml/min^{-1}. With the solid state electrochemical devices continually monitoring the argon the furnace was gradually ($\sim$2 days) brought to the operating temperature ($\sim$1300°C). After adsorbed gases had been removed then both oxygen monitors indicated that the flow of purified argon could establish an "equivalent" oxygen partial pressure of 10^{-15} to 10^{-18} atm within the alumina reaction tube. When such conditions prevailed the pure iron container was gradually introduced into the hot zone and an investigation into the appropriate oxycarbide system carried out. Further confirmation of the low oxygen chemical potentials established in the purified argon atmosphere was provided by the absence of oxide films* on the pure iron container when the latter was examined after it had been rapidly withdrawn from the hot zone at the completion of a run which usually lasted about 200 h.

The preceding state of affairs, however, was realized only occasionally, and in general the tubes deteriorated very rapidly, making it impossible to maintain a sufficiently low oxygen

---

*The oxygen partial pressure in equilibrium with Fe and FeO at 1300 and 600°C is approximately 10^{-11} and 10^{-19} atm, respectively.

TABLE I Summary of behaviour of alumina tubes

Tube no.	Vacuum*		Length of time at 1300°C (h)	Length of time at 1300°C in argon atm (h)	Inlet oxygen partial pressure p_{O_2} (atm)	Outlet oxygen partial pressure p_{O_2} (atm)	Comments
	Cold (torr)	Hot (1300°C) (torr)					
1	38×10^{-3}	47×10^{-3}	520	350[a]	—[b]	—[b]	Slight tarnishing of Fe crucible commenced in region maintained at 1000°C (p_{O_2} 10^{-15} atm). Failure due to cracking when vacuum testing hot tube.
2 (i)	40×10^{-3}	45×10^{-3}	1300	160[a]	—[b]	—[b]	Slight tarnishing of Fe crucible suggested that p_{O_2} was 10^{-15} atm. Experiment completed.
(ii)	—	—		178	—[b]	—[b]	As above.
(iii)	—	—		178	10^{-20} (initial) 10^{-16} (final)	$10^{-16.5}$ (initial) 10^{-16} (final)	Slight tarnish on Fe crucible at 950°C Experiment completed.
(iv)	—	47×10^{-3}		250	10^{-18} 10^{-17}	$10^{-18.2}$ 10^{-17}	Experiment completed.
(v)		300×10^{-3}					Unable to obtain low vacuum. Furnace slowly cooled and subsequent examination of tube revealed hair-line cracks in hot zone.
3 (i)	55×10^{-3}	55×10^{-3}	80				A long time (3 h) required to attain reported vacuum. No iron crucible inserted, and tube not filled with argon.
(ii)		1000×10^{-3}					Subsequent examination of tube indicated high-temperature porosity. When cold the vacuum recorded was 75×10^{-3} torr.
4	40×10^{-3}	80×10^{-3}	100	24	10^{-21} 10^{-20}	$10^{-17.2}$ 10^{-9}	The run was terminated due to the relatively high outlet p_{O_2} recorded. Subsequent examination revealed hair-line crack in hot-zone.
5 (i)	40×10^{-3}	—[c]	1900	72	10^{-17} 10^{-16}	10^{-17} $10^{-17.3}$	Experiment completed.
(ii)	—	—		250	10^{-18} 10^{-17}	10^{-20} $10^{-16.5}$	Experiment completed.
(iii)		—		154	$10^{-17.5}$ $10^{-16.4}$	10^{-18} 10^{-16}	Slight tarnishing of Fe crucible commencing in region corresponding to a temperature of 850°C. Experiment completed.
(iv)		—		104	10^{-19} $10^{-16.6}$	$10^{-19.2}$ $10^{-17.5}$	Experiment completed.
(v)				120	10^{-18} 10^{-19}	$10^{-17.5}$ $10^{-16.7}$	Experiment completed.
(vi)				16	10^{-18} 10^{-19}	10^{-12} 10^{-10}	Experiment terminated due to relatively high oxygen partial pressure recorded by outlet monitor. Subsequent examination of the tube revealed development of porosity as described in the present paper.

*The values reported for the pressure were those recorded after pumping the system for approximately ½ h and refer to "dynamic" conditions with the system still being evacuated by the pumps.

[a] During the initial experiments the argon was "gettered" by passing the gas through a bed of Ti granules in an external furnace maintained at 750 to 800°C. In all subsequent experiments additional Ti granules were placed within the reaction tube as indicated in Fig. 1.

[b] Oxygen monitors were not employed during the initial experiments.

[c] Vacuum testing of the heated tubes was stopped as this procedure might have been responsible for the development of the hair-line cracks found in tubes 1 and 4.

chemical potential within the reaction tube. The behaviour of five tubes examined over a period of eighteen months is summarized in Table I. In an attempt to elucidate the mechanism involved in the failure of these impermeable pure alumina components one of the tubes was subjected to a variety of examinations which are reported in the following sections.

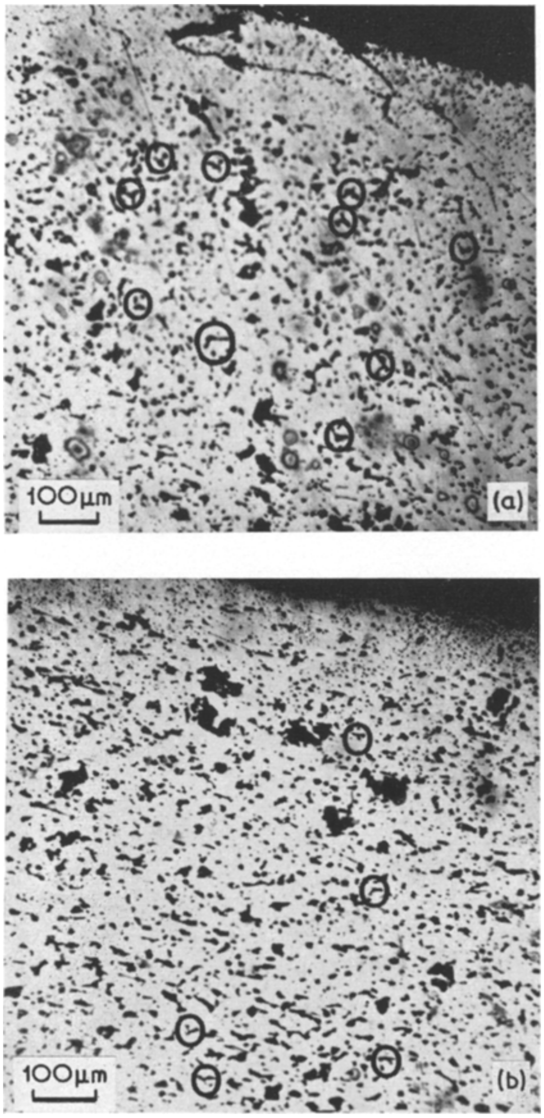

Figure 2 (a) Polished inner wall section of hot zone showing porosity connecting surface interior (normal to tube axis). (b) Polished inner wall section of cold zone (normal to tube axis).

2.2. Light microscopy

Sections taken from the hot and cold regions of the tube, were mounted and polished as described elsewhere [8]. Typical micrographs are illustrated in Figs. 2a and b, and occasional fissures connecting the surface of the inner wall to the tube interior are clearly visible on the hot-zone sample. There is also some indication that the number of voids located at the junction of three grains (identified by the circles in Fig. 2) is greater in the hot-zone sample.

More details of the microstructure were revealed, as shown in Figs. 3a and b, by thermally etching the polished sections in air for 8 min at 1600°C using a molybdenum furnace. A surface "skin" containing very large (~500 µm) orientated alumina grains can be seen, and it appears [1, 2] that the presence of this type of surface skin is a feature of many sintered oxide products fabricated by an extrusion process, and is certainly typical of all the alumina tubes used in the present investigation which were supplied

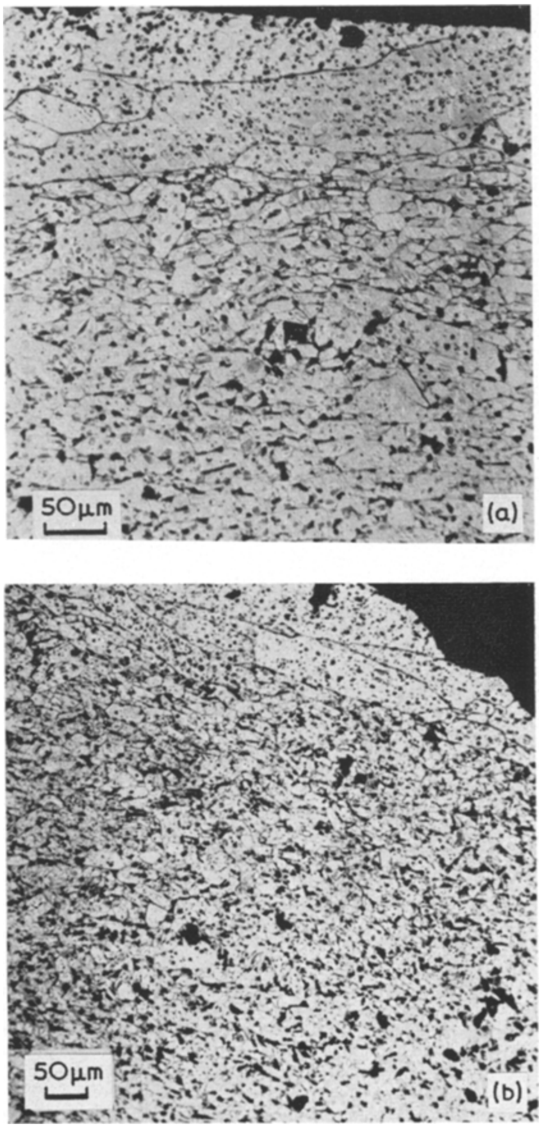

Figure 3 (a) Thermally etched inner wall section of hot zone showing grain growth relative to cold-zone sample. (b) Thermally etched inner wall section of cold zone.

by the same firm. The average grain-size, calculated by the method reported by Fullman, was 16 μm in the interior of the hot-zone sample, compared to 14 μm in the cold-zone sample which suggests that significant grain growth has occurred during the 700 h the tube was in service at 1300 °C. It should also be noted that there is extensive intra-granular porosity in the large grains associated with the surface skin, and there is possibly some evidence for a greater incidence of such pores in the sample taken from the hot zone.

The micrographs obtained by thermal etching only appeared as shown in Figs. 3a and b after they had been soaked in HF for $\frac{1}{2}$ h. Initial examination of the sections before HF treatment revealed a microstructure contaminated with "drops" of a glassy phase as shown in Fig. 4. It was originally considered that this contamination came from the walls of the alumina reaction tube in the molybdenum furnace, or from the alumina crucible containing the sample during the thermal etching procedure. However, the incorporation of a lid on top of the alumina crucible, or its complete replacement by a closed thoria crucible, failed to prevent the formation of the thin glassy regions. It was concluded, therefore, that the contamination probably originated from within the sample itself. Although a number of acids were tried, HF was the only solvent that effectively removed the contamination which was assumed to be a glassy silicate phase derived from the silica content of the sample.

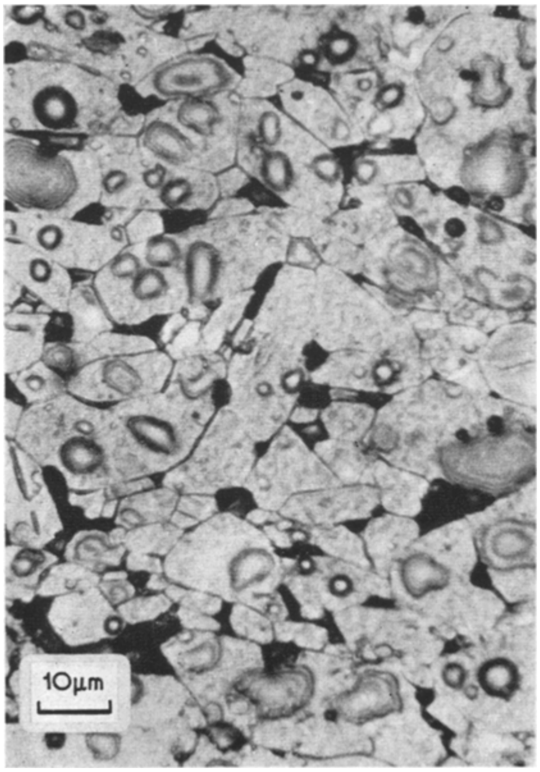

Figure 4 Thermally etched section showing glassy surface pools.

2.3. Scanning electron microscopy

Scanning electron micrographs, taken at 25 kV, of gold-coated fracture samples are shown in Fig. 5. The structure of the inner surface skin in the hot (Fig. 5a) and cold (Fig. 5b) zone can be compared and it appears that there are more elongated large pores in the sample obtained from the hot zone. The smaller size of the grains in the interior of the wall of the tube is evident from the next two micrographs but there is little obvious difference between the hot (Fig. 5c) and cold (Fig. 5d) zone samples.

2.4. Electron probe analysis

The amounts of Mg, Mn, Cr, K and Na present were too small to be detected by the instrument. The iron concentration was reported to be 250 ppm, and the silicon concentration 3000 ppm, in both hot- and cold-zone samples. The calcium content was given as about 250 ppm in the hot zone and 580 ppm in the cold zone. It is interesting to note that the distribution of the silicon and calcium was similar and was often concentrated in the vicinity of pores. The value for silicon content obtained by this method appears to be too high and has been ignored in subsequent discussions.

2.5. Chemical analysis

Wet chemical analysis were carried out at the British Ceramic Research Association on samples taken from hot and cold zones, and the following results reported. The values are in accordance with previously reported data [1] for similar tubes.

Additional spectrographic analysis performed at Imperial College (Analytical Services Laboratory) gave an estimated 55 ppm Na_2O and 95 ppm Na_2O in the hot and cold zones respectively.

2.6. Density determinations

Densities of two samples taken from both hot

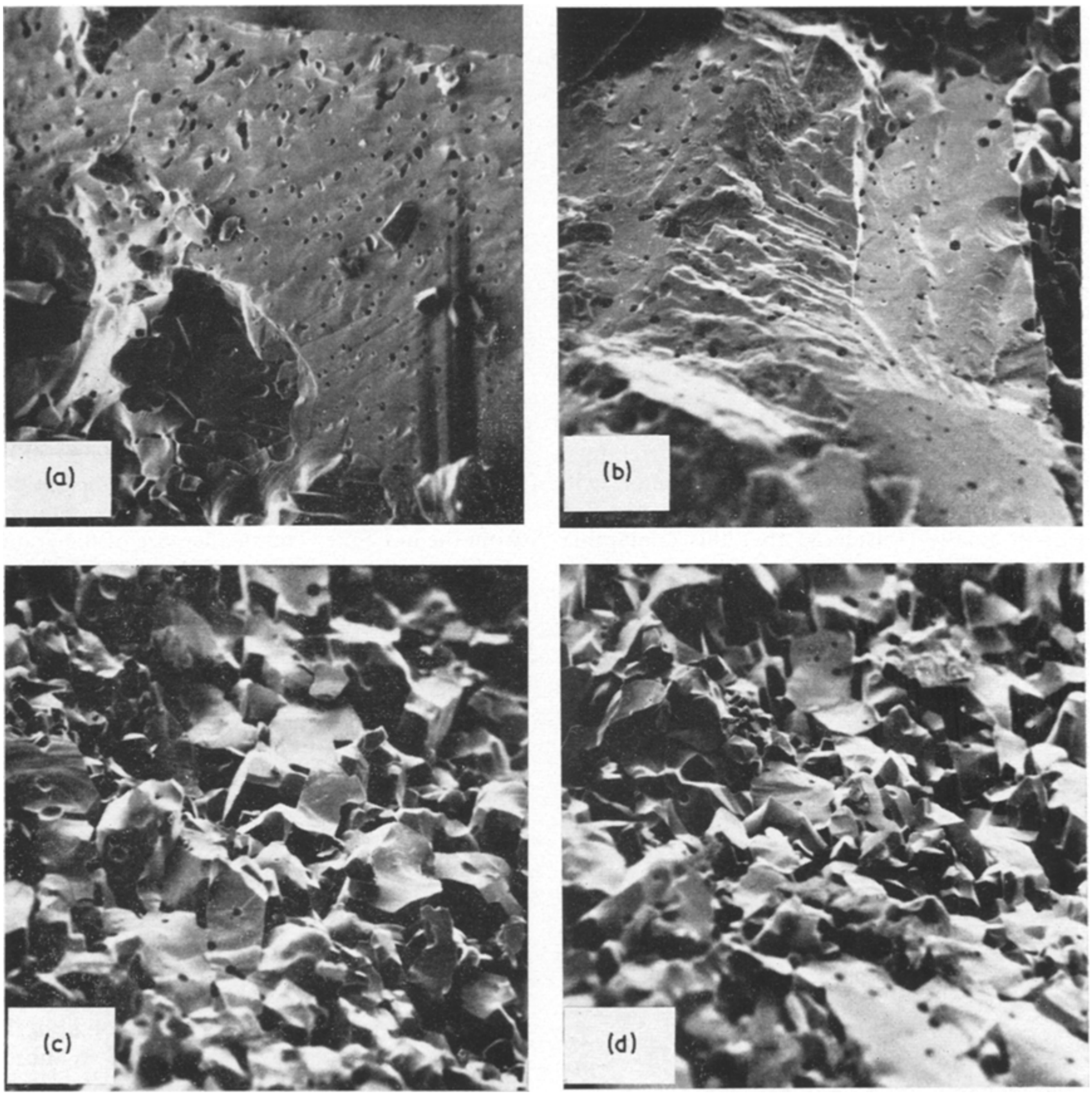

Figure 5 (a) Scanning electron micrograph of the inner edge of a fractured surface in the hot zone (normal to tube axis). (b) Scanning electron micrograph of the inner edge of a fracture surface in the cold zone (normal to tube axis). (c) Scanning electron micrograph of hot-zone tube interior (normal to tube axis). (d) Scanning electron micrograph of cold-zone tube interior (normal to tube axis). All × 630.

and cold zones were obtained using a mercury densitometer. Measurements were carried out on fractured specimens weighing approximately 1 g. Seven readings were taken for each specimen, and the procedure was also verified by measuring the density of single crystal alumina. Temperature corrections were applied to the mercury density in all cases.

2.7. Dye impregnation

$1\frac{1}{2}$ in. long sections from the hot and cold zones of the tube were carefully degreased and dried overnight at 120°C. Vacuum impregnation with a fluorescent dye* was then carried out in an apparatus similar to that described by Fryer and Roberts [9]. After 35 min, the specimens were removed, broken

---

*Zyglo Penetrant Z1 supplied by Solus-Schell, Stanmore, Middlesex.

Oxide	Cold-zone analysis (wt %)	Hot-zone analysis (wt %)
SiO_2	0.09	0.04
CaO	0.07	0.05
MgO	0.01	<0.01
K_2O	<0.01	<0.01
Na_2O	<0.01	<0.01

	Density g cc^{-1}	
	1st specimen	2nd specimen
Hot zone	3.63	3.62
Cold zone	3.67	3.68

carefully parallel to the tube axis with a hammer and chisel, and the sections were then photographed under ultra-violet light. A typical result is shown in Fig. 6 where the extent of the dye penetration is revealed by the white regions. It is evident that no detectable penetration has occurred into either wall of the cold zone specimen (right), nor into the outer wall of the hot specimen (left). Penetration into the inner wall of the hot-zone sample, however, is clearly visible. It should also be noted that extensive penetration into the interior of the wall has occurred from the ends of the samples. This degree of penetration cannot be attributed to mechanical damage produced when the samples were cut from the original tube.

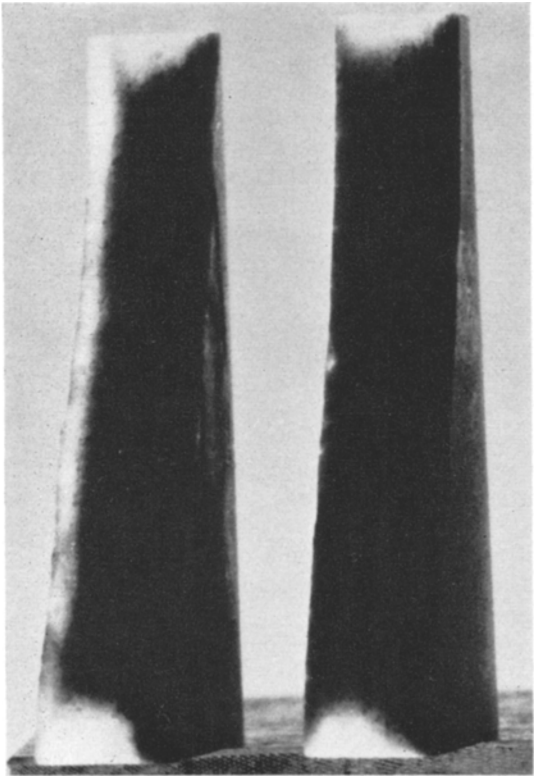

Figure 6 Dye impregnation of hot and cold zone wall sections parallel to tube axis (hot section on left).

3. Discussion

Examination of appropriate specimens using the dye impregnation technique indicated that the outer surface of the tube from both cold and hot zones was impermeable as was also the inner surface of the cold-zone sample. The inner surface from the hot zones, however, appeared to be highly permeable, and it should also be noted that the dye was able to penetrate into the interior of the wall from the transverse section produced when the sample was cut from the tube. Thus, although porosity had developed within the inner surface during the high-temperature operation of the tube, the overall wall section remained impermeable (at least to the liquid dye) and yet sufficient oxygen was entering the reaction tube to make it impossible to establish the required low oxygen partial pressures ($\sim 10^{-15}$ atm).

The micrographs in Figs. 3 and 5 indicated that the development of porosity in the inner surface layer was associated with the appearance of occasional fissures connecting the surface to the interior, and also with an increased number of large elongated pores within the grains. These features can be attributed to the volatilization of impurities (SiO_2, CaO, Na_2O) in accordance with the data provided by the chemical analysis, and also the earlier reports of Roberts *et al* [1]. The inner surface skin incorporating the large orientated grains is only about 100 μm wide (approximately, 1/50 of the total wall thickness) and so cannot be solely responsible for the decrease in total SiO_2 content of over 50%, and it follows that SiO_2 must also be lost from the interior region of the wall section. As already noted there is evidence from Fig. 2 that the number of voids located at the junction of three grains within the interior is greater in the hot-zone sample, and it is possible that these voids are part of an interconnecting network of channels which allow the volatile constituents to permeate to the inner surface of the tube. It should be recalled that permeability of the interior region in both hot and cold zone samples was inferred from the dye impregnation test.

Thermodynamic analysis using values taken from Kubaschewski *et al* [10] confirm that SiO_2 could be transported as a volatile species according to this reaction:

$$2\ SiO_2\ (s) \rightleftharpoons 2\ SiO\ (g) + O_2\ (g)\ .$$

For a temperature of 1320°C, the equilibrium constant, has a value of 10^{-25}, i.e.

$$K = \frac{p_{SiO}^2\ p_{O_2}}{a_{SiO_2}^2} = 10^{-25}\ .$$

Assuming the activity of SiO_2 to be unity and the oxygen partial pressure established within the reaction tube to be 10^{-18} atm then $p_{SiO} = 3 \times 10^{-4}$ atm (0.23 torr). This pressure of silicon monoxide could certainly account for the removal of SiO_2. For example, assuming saturation at 1320°C then an argon flow rate of 100 ml min^{-1} would remove approximately 1 mg of SiO_2 per hour. According to this rate of removal in the hot zone a section of the tube weighing 100 g (about 10 cm long) could have its SiO_2 content reduced from 0.09 to 0.04% in 50 h thus explaining the results obtained by chemical analysis (Section 2.3). These calculations obviously represent the maximum rate of SiO_2 removal as they assume saturation of the argon and ignore the kinetic factors such as the rate of permeation of the silicon monoxide gas through the channels produced in the surface skin of the inner wall. It is also implicit in the calculations that the SiO_2 and other impurities are principally concentrated along grain boundaries and pores rather than generally distributed within the alumina grains. The X-ray microprobe results provided some evidence for this assumption which is also supported by the work of Jorgensen and Westbrook [11].

The analysis does focus attention onto effects which can be produced by the establishment of low oxygen partial pressures in commercial alumina tubes. These effects at moderate temperatures can certainly be more deleterious than the application of vacuum conditions (e.g. 10^{-5} torr) which probably correspond, in the absence of getters, to oxygen partial pressures around 10^{-8} atm. Under these conditions p_{SiO} would be approximately 3×10^{-9} atm and the corresponding maximum weight loss due to volatilization of SiO_2 according to the Hertz-Knudsen equation would be 3.8 mg h^{-1} cm^{-2}. However, the area available for free evaporation of the SiO_2 would be considerably less than 1 cm^2, and it can be concluded that vacuum conditions would be less exacting than the imposition of low oxygen partial pressures around 1300°C.

It might be argued that the activity of SiO_2 will not be unity as it is probably combined with Na_2O, CaO, Al_2O_3 to form glassy impurities in the pores and grain boundaries. However, silica is the principal impurity, and providing the silica content of the glass does not fall much below 50 mol% then available thermodynamic data [12] on silicate systems indicates that the silica activity is expected to be around unity. It is also relevant to note that a recent paper by Davis *et al* [19] has attributed the decomposition of mullite ($2\ Al_2O_3 . SiO_2$) at high temperatures to the formation of gaseous SiO at the low oxygen partial pressures imposed in the experimental conditions.

A similar analysis can be attempted for the loss of CaO according to the reaction,

$$2\ CaO\ (s) \rightarrow 2\ Ca\ (g) + O_2\ (g)\ .$$

At 1320°C,

$$K = \frac{p_{Ca}^2 \cdot p_{O_2}}{a_{CaO}^2} = 1.7 \times 10^{-32}\ \cdot$$

Inserting the values, $A_{CaO} = 1$, and $p_{O_2} = 10^{-18}$ atm then the equilibrium calcium vapour pressure is 1.3×10^{-7} atm. This low value cannot explain the loss of calcium in the hot zone indicated by the chemical analysis results. It is, however, possible to postulate reactions involving the formation of silicates such as calcium orthosilicate according to the reaction:

$$3\ CaO\ (s) + SiO_2\ (s) \rightarrow Ca\ (g) + Ca_2SiO_4\ (s) + \tfrac{1}{2}O_2\ (g)\ .$$

At 1593 K

$$K = \frac{p_{Ca} \cdot a_{Ca_2SiO_4} \cdot p_{O_2}^{\frac{1}{2}}}{a_{CaO} \cdot a_{SiO_2}} = 2 \times 10^{-12}\ \cdot$$

Assuming all the condensed phases are present at unit activity and $p_{O_2} = 10^{-18}$ it follows that $p_{Cc} = 2 \times 10^{-3}$ atm. A calcium vapour pressure of this magnitude could easily account for the decrease in the calcium content of the hot-zone samples.

A similar situation would also prevail for any MgO present except that the magnesium vapour pressures would be even higher, and in fact the overall mechanism can be compared to the production of magnesium from magnesia by means of the Pidgeon process [13].

The thermodynamic calculations also suggest the following comments. A commercial alumina tube operated under conditions similar to those described earlier ($p_{O_2} \sim 10^{-18}$ atm) could result in significant contamination of samples undergoing heat-treatment due to the volatilization of SiO_2 ($\sim$ 1 mg h^{-1}). It would also appear that the introduction of silicon or silica components within the reaction tube should significantly decrease the loss of silica from the walls of the tube as the components would themselves establish the appropriate p_{SiO} pressure [14]. Under these conditions deterioration of the tube should be slower, and it would be interesting to know, for example, whether alumina reaction tubes used in the production of Si_3N_4 are less susceptible to failure due to the development of permeability.

Although the development of porosity in the surface skin of the inner wall and decrease in impurity content can be explained by the formation of volatile species there still remains the problem of the surface skin on the outer wall. At 1700°C with the inside of the tube exposed to vacuum conditions and air on the outside Dhavale's [15] results indicated that the outer skin also occasionally developed very small fissures or channels. These were not revealed by the fluorescent dye impregnation test but by another type of examination in which samples were exposed to tin chloride vapour. Subsequent X-radiographic examination showed that the vapour had occasionally been able to penetrate the outer skin along micro-fissures. It is, of course, possible that micro-fissures also developed in the outer wall of samples examined during the present investigation and which were not detected by the fluorescent dye technique. However, for the conditions prevailing in Dhavale's experiments, volatilization of the impurities alone could account for their removal, whereas at the lower temperatures encountered in the present investigation the formation of gaseous species was associated with the imposition of the low oxygen partial pressure. In the region of the outer surface skin the oxygen partial pressure would be higher as the exterior wall of the tube was in contact with the surrounding air. Volatilization of impurities from this region would be less and it is probable that the associated micro-fissures would not be generated. It is suggested, therefore, that the inability to maintain a low oxygen partial pressure within the reaction tube is due to diffusion rather than permeation through the relatively thin impermeable surface region at the outer wall. It is relevant to note that the chemical diffusion coefficient [16] in single crystal sapphire is about 10^{-8} cm^2 sec^{-1} at 1400°C. This is the effective diffusion coefficient [17] when transport is occurring as the result of a concentration gradient and is many orders of magnitude greater than the self-diffusion coefficient [18] of Al^{3+} in single crystal Al_2O_3 (3×10^{-14} cm^2 sec^{-1} at 1400°C). The corresponding transport processes through the thin (100 μm) polycrystalline outer surface skin will be further enhanced by grain-boundary diffusion and are probably responsible for the inability to maintain low oxygen partial pressures within the reaction tube once the inner surface skin has become permeable.

4. Conclusions

The inability to maintain low oxygen partial pressures within impermeable commercial alumina tubes at moderate temperatures (~1300°C) was attributed to the development of porosity in the surface skin of the inner wall. Chemical analysis indicated that this porosity was associated with a decrease in the impurity content of hot-zone samples, and thermodynamic analysis confirmed that the relevant quantities of SiO_2, CaO, MgO would be removed as volatile species generated by the imposed low oxygen partial pressures. Chemical diffusion of oxygen through the remaining thin outer wall skin would then be of sufficient magnitude to prevent the establishment of low oxygen partial pressures except for well-buffered atmospheres. The thermodynamic analysis also suggested that the mechanism responsible for the development of porosity and ultimate failure of the alumina tubes is not identical for operation at moderate temperatures with low oxygen partial pressures and for operation at high temperatures under vacuum conditions. It could also be concluded that the development of porosity at the low oxygen partial pressures established in "inert" atmospheres could be retarded by the introduction of components which would establish appropriate partial pressures of silicon monoxide and calcium within the reaction tube.

Acknowledgements

The results reported were obtained during an investigation supported by AERE, Harwell into the thermodynamic properties of oxycarbide phases. The writers also wish to acknowledge discussions with Dr E. W. Roberts, Ceramics Department, Leeds University, which contributed to the interpretation of the microstructural features.

References

1. D. HAYES, D. W. BUDWORTH, and J. P. ROBERTS, *Trans. Brit. Ceram. Soc.* **62** (1963) 507.
2. J. P. ROBERTS, in "Ceramic Microstructures", eds. R. M. Fulrath and J. A. Pask (Wiley, New York, 1968) p. 509.
3. K. SCHWERDTFEGER and R. T. TURKDOGAN, in "Physicochemical Measurements in Metals Research" (ed. R. A. Rapp) p. 321; vol. IV, Part I in "Techniques of Metals Research" (ed. R. F. Bunshah) (Wiley Interscience, New York, 1970).
4. Y. JEANNIN, C. MANNERSKANTZ, and F. D. RICHARDSON, *Trans. AIME* **227** (1963) 300.
5. B. C. H. STEELE, N. A. JAVED, and C. B. ALCOCK, *J. Nuclear Mats.* **35** (1970) 1.
6. B. C. H. STEELE, in "Heterogeneous Kinetics at Elevated Temperatures" (Plenum Press, New York, 1970) p. 135.
7. B. C. H. STEELE and Electronic Instruments Ltd, British Patent 42576/69.
8. M. A. WILLIAMS, Ph.D. Thesis, University of London, 1971.
9. G. M. FRYER and J. P. ROBERTS, *Trans. Brit. Ceram. Soc.* **62** (1963) 537.
10. O. KUBASCHEWSKI, E. LL. EVANS, and C. B. ALCOCK. "Metallurgical Thermochemistry", 4th edn. (Pergammon, London, 1967).
11. P. JORGENSEN and J. WESTBROOK, *J. Amer. Ceram. Soc.* **47** (1964) 334.
12. R. SRIDHAR and J. H. E. JEFFES, *Trans. Inst. Min. Metall. Sect. C* **78** (1969) C 14.
13. L. M. PIDGEON and J. A. KING, *Discuss. Faraday Soc.* no. 4 (1948) 197.
14. S. WILD, P. GRIEVESON, and K. H. JACK. In "Metallurgical Chemistry" (ed. O. Kobaschewski) (H.M.S.O., London, 1972) p. 339.
15. A. K. DHAVALE, Ph.D. Thesis, Leeds University, 1970.
16. T. P. JONES, R. L. COBLE, and C. J. MOGAB, *J. Amer. Ceram. Soc.* **52** (1969) 331.
17. P. E. CHILDS, L. W. LAMB, and J. B. WAGNER, *Proc. Brit. Ceram. Soc.* **19** (1971) 29.
18. A. E. PALADINO and W. D. KINGERY, *J. Chem. Phys.* **37** (1962) 957.
19. R. F. DAVIS, I. A. AKSAY, and J. A. PASK, *J. Amer. Ceram. Soc.* **55** (1972) 98.

Received 21 August and accepted 1 September 1972.